Investigation of the effect of DC electric field on a small ethanol diffusion flame

Yanlai Luo [1], Yunhua Gan [1,*], Xi Jiang [2,**]

1. School of Electric Power, South China University of Technology, Guangdong 510640, China;

2. Engineering Department, Lancaster University, Lancaster LA 1 4YR, UK

*Corresponding author: Prof. Yunhua Gan, Ph.D.,

Address: School of Electric Power, South China University of Technology, Wushan Road, Tianhe

District, Guangzhou 510640, China

Tel/Fax: 00-86-20-87110613

Email: ganyh@scut.edu.cn.

**Corresponding author: Prof. Xi Jiang, Ph.D.,

Address: Engineering Department, Lancaster University, Lancaster LA 1 4YR, UK

Tel/Fax: 00-44-1524592439

Email: x.jiang@lancaster.ac.uk.

ABSTRACT

A small ethanol diffusion flame exhibited interesting characteristics under a DC electric field. A numerical study has been performed to elucidate the experimental observations. The flow velocity, chemical reaction rate, species mass fraction distribution, flame deformation and temperature of the flame in the applied DC electric field were considered. The results show that the applied electric field changes the flame characteristics mainly due to the body forces acting on charged particles in the electric field. The charged particles are accelerated in the applied electric field, resulting in the flow velocity increase. The effects on the species distribution are also discussed. It was found that the applied electric field promotes the fuel/oxidizer mixing, thereby enhancing the combustion process and leading to higher flame temperature. Flame becomes shorter with applied electric field and its deformation is related to the electric field strength. The study showed that it is feasible to use an applied DC electric field to control combustion and flame in small-scale.

1   **Nomenclature**

2

c_P	constant-pressure specific heat capacity
D	diffusivity
d_i	inner diameter of burner nozzle
d_o	outer diameter of burner nozzle
E	electric field strength
e	electron charge
F	body force
H	height of flame
h_i	enthalpy of species i
$\boldsymbol{J}_i$	diffusive flux of species i
k	effective heat transfer coefficient
L	electrode spacing
n_c	net charge density
n_+	positive charge density
n_-	negative charge density
p	pressure on the element
r	radial direction
R	correlation coefficient
R_e	radius of electrode
R_i	net reaction rate of species i

S_h volume heat source term

S_i additional generation rate caused by source terms

T flame temperature

u axial (x) direction of flow velocity

v radial (r) direction of flow velocity

W width of flame

Y_i mass fraction of species i

Greek Letters

α aspect ratio

μ dynamic viscosity

ρ density of liquid ethanol

τ viscous dissipation stress

1

1. Introduction

The characteristics of micro- and meso-scale combustors with different configurations or under different external conditions have attracted lots of attention, e.g. [1-5]. The effects of an electric field applied on flame have been studied recently, e.g. [6-9]. Researchers found that the electric field can improve the stability of combustion. The external electric field was also used as a means for flame control, such as taking flame as an electrically active component based on voltage-current characteristics in the circuit [10]. The effects of electric fields on flame included stabilizing the combustion, increasing flame speed, reducing the soot production and emission, changing the flame temperature and shape [11-15]. These findings also imply that the efficiency of practical non-premixed combustion systems could be improved by applying an electric field [16]. It has been identified that there are three major effects produced by the electric field on the flame, including the thermal effect, the ionic wind effect and the electrical-chemical effect [17].

Experimental and numerical methods have been used to study the effects of electric fields on flame behavior. Meng et al. [18] found that the flame propagation and combustion properties were significantly affected by the DC electric fields and the flame shape would become a prolate spheroid by the electric body force in the electric field. Imamura et al. [19, 20] investigated the flame deformation of ethanol droplets in different vertical electric fields experimentally and the relation between the applied voltage and electrode distance was observed. Kim et al. [21] considered the stabilization characteristics of liftoff and blowoff in nonpremixed laminar jet flames in a coflow for propane fuel by applying AC and DC electric fields experimentally. Boom et al. [22] studied the influence of a DC electric field on the laminar burning velocity and found that the electrode configuration can influence the laminar burning velocities and the system requires a relatively low

power input. Belhi et al. [23] improved a simplified mathematical model, where negative ions and the stabilization mechanism of a diffusion lifted flame in the applied DC or AC electric fields were analyzed. The effects of electric fields on the reattachment of lifted flames have been investigated experimentally by Won et al. [24] and they reported that the stabilization limit of attached flames was extended by the AC electric field and the effect of DC was found to be minimal. Karnani and Dunn-Rankin [25] discussed the relationship among flame shape, combustion intensity, soot formation, and the ion production rate. They found that those parameters are related to the voltage–current relationship for a coflowing non-premixed methane/air flame. Vega et al. [26] studied the electro-physical means of controlling the nitrogen oxide pollutant formation and emission composition of premixed flames in the combustion process.

Most of these studies considered hydrocarbon fuels, especially gaseous fuels. Although diffusion flames with liquid fuels are important in terms of the effects of electric fields on combustion phenomena, the investigation is limited in the literature and there is still a lack of understanding on this topic. A small ethanol diffusion flame with an applied electric field was investigated in this study, investigating the effects of electrical field on combustion and the potential application in system control. The effects of DC electric field on the flame characteristics, such as flame shape, temperature, species distribution, flow velocity and reaction rate, were investigated experimentally and numerically. The combined experimental and numerical results enhance the understanding of the effects of electric field on the small ethanol diffusion flame. When small combustors are considered in transport applications such as a drone, liquid fuel is preferred because of the very large energy density (in comparison to gas fuels). The results and understandings obtained can be used to improve the performance of meso-scale combustors controlled using

electrical fields.

2. Experiment

2.1 Experimental system

The schematic of experimental apparatus and a simplified electrical circuit are shown in Fig. 1. The system consists of four main parts, including liquid fuel supply system, small-scale combustion system, DC power supply system and measurement system. The fuel used in these experiments was high purity ethanol (C_2H_5OH, molecular weight of 46.07, purity $> 99.5\%$) and it was controlled and supplied from the base into the burner nozzle with an inner diameter (d_i) of 0.9 mm and outer diameter (d_o) of 1.2 mm by a syringe pump (KDS 100) with an uncertainty of 1.0%. Air around the burner nozzle as the oxidizer was supplied from the ambient. The flame was ignited near the nozzle outlet and was located between two parallel horizontal brass plate electrodes with radius (R_e) of 40 mm. A potential difference applied by a DC power supply (Boher HV, Model 71030P) between the two electrodes produced the DC electric field. The measurement system consisted of digital camera (Cannon, EOS 5D Mark Ⅲ) to observe the flame shape, S type platinum-rhodium thermocouple with the node diameter of 0.3 mm, and data acquisition instrument (Agilent, 34970A) to measure the flame temperature, which also could collect data of current and voltage. The system is similar to that used in our previous work [27-29].
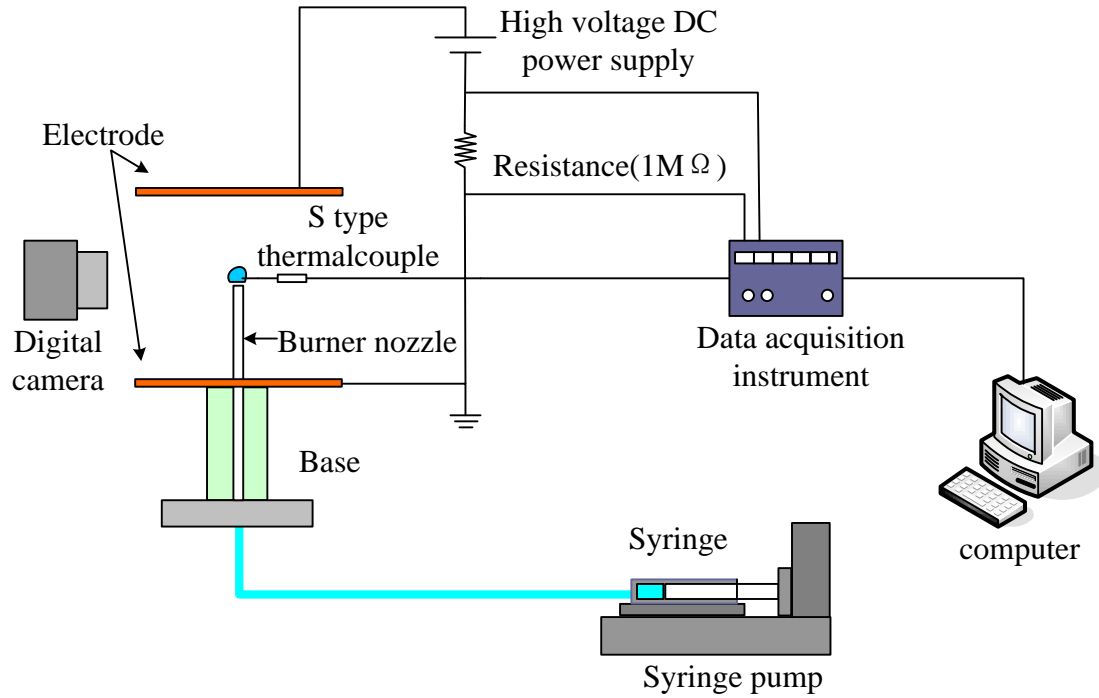
Fig. 1 Experimental system

2.2 Experimental method

The applied voltage, normalized electrode spacing L, the nominal electric field strength (E) are the key electrical parameters to describe the system. A positive electric field is defined as electric field vectors directed from the burner to the downstream electrode and reversely negative. When the power supply voltage or electrode distance was changed, the electric field strength would change accordingly and some different electric field conditions were produced. A small-scale diffusion flame in different electric field conditions was observed and the data such as flame shape, temperature variation and flow velocity were collected. These cases were compared and analyzed, and the effects of DC field on small-scale diffusion flame combustion characteristics were examined.

A thermocouple was used to measure the flame temperature at the flame top position, as shown in Fig. 2. The flame temperatures at different positions were measured and it was found that the highest temperature in the flame was at the top position. So the temperature at the top position was chosen to

represent the flame temperature. Moreover, the measurement at the top position brought the smallest disturbance to the flame compared with other positions [28].
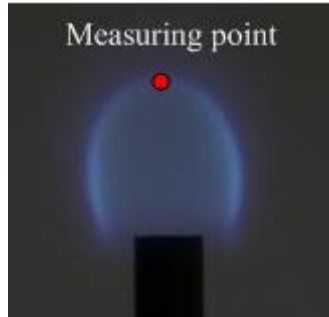

Fig. 2 Flame temperature measuring point

3. Model description

3.1 Geometric and mathematical model

Fig. 3 shows a schematic of the axisymmetric model of the small-scale combustor with two plate electrodes. The model scale depended on the actual experimental system. In the experiments, electrode spacing had been adjusted to 40 mm. The upper electrode was connected to the high voltage of the power supply as the anode and the upper electrode was connected to the low voltage as the cathode. In consideration of the domain symmetry, a half of the cross-section of the domain was selected in the axisymmetric model to reduce the computational cost.
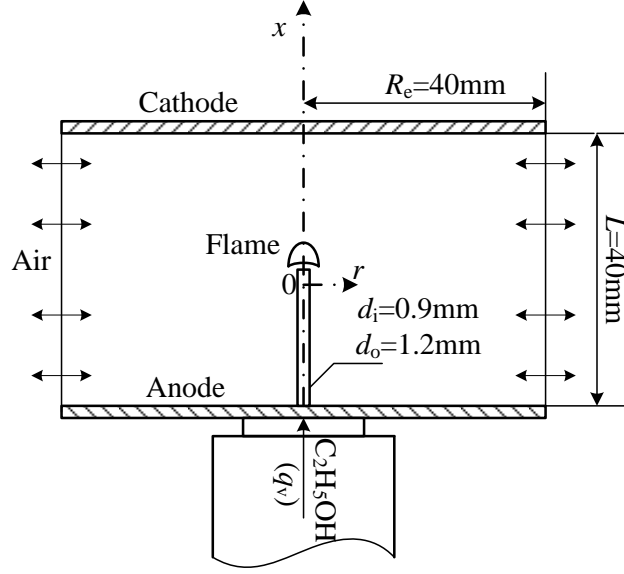
Fig. 3 The configuration studied

Since the main focus of the study was on the steady mean flow field, only steady and axisymmetric numerical simulations were considered. The mixture flow and combustion process followed conservation equations including the continuity, momentum, energy and species conservations for the governing equations.

In steady state, the governing equations of axisymmetric cylindrical coordinates are presented as follows:

Continuity:

$$\frac{\partial(\rho u)}{\partial x} + \frac{1}{r}\frac{\partial(r\rho v)}{\partial r} = 0 \tag{1}$$

where ρ is the density of flow, u is the x direction of flow velocity, and v is the r direction of flow velocity.

Momentum:

x direction:

$$\frac{\partial(\rho uu)}{\partial x} + \frac{1}{r}\frac{\partial(r\rho uv)}{\partial r} = -\frac{\partial p}{\partial x} + 2\frac{\partial}{\partial x}(\mu\frac{\partial u}{\partial x}) + \frac{1}{r}\frac{\partial}{\partial r}(r\mu\frac{\partial u}{\partial r}) + \frac{1}{r}\frac{\partial}{\partial r}(r\mu\frac{\partial v}{\partial x}) + F_x \tag{2}$$

r direction:

$$\frac{\partial(\rho uv)}{\partial x} + \frac{1}{r}\frac{\partial(r\rho vv)}{\partial r} = -\frac{\partial p}{\partial r} + \frac{\partial}{\partial x}(\mu\frac{\partial v}{\partial x}) + \frac{\partial}{\partial x}(\mu\frac{\partial u}{\partial r}) + \frac{2}{r}\frac{\partial}{\partial r}(r\mu\frac{\partial v}{\partial r}) + \frac{2\mu v}{r^2} + F_r \tag{3}$$

where μ is the dynamic viscosity, p is the pressure on the flow element, and F_x, F_r are the body

force on the element.

The source term of momentum equation in the axial direction is given as:

$$F_x = F_e = Ee(n_+ - n_-) = Een_c \tag{4}$$

where e is the electron charge, n_+ is the positive charge density, n_- is the negative charge density,

and n_c is the net charge density.

The model was simplified and the net charge density was considered. The number of charged

particles was estimated according to the literature (10^9-10^{12} cm^{-3}) [17-19]. According to Equation (4),

the electric field force was estimated as

$$F = Een_c = 1600 \text{ N/m}^3, E=100 \text{ kV/m}, n_c=10^{11}\text{cm}^{-3}$$

which is similar to the results in the literature (0-2000 N/m^3) [21].

Energy:

$$\frac{\partial}{\partial x}(\rho uh_i) + \frac{1}{r}\frac{\partial}{\partial r}(r\rho vh_i) = \frac{\partial}{\partial x}(\frac{k}{c_P}\frac{\partial h_i}{\partial x}) + \frac{1}{r}\frac{\partial}{\partial r}(r\frac{k}{c_P}\frac{\partial h_i}{\partial r}) - \frac{\partial(h_i J_i)}{\partial x} - \frac{1}{r}\frac{\partial(h_i J_i)}{\partial r} + \frac{\partial(\tau u)}{\partial x} + \frac{1}{r}\frac{\partial(r\tau v)}{\partial r} + S_h$$

$$\tag{5}$$

where k is effective heat transfer coefficient, h_i is the enthalpy of the species i, J_i is the

diffusive flux of the species i, c_P is the constant-pressure specific heat capacity of the mixture, the

temperature, τ is the viscous dissipation stress, and S_h is the volumetric heat source term.

In our previous work [28], it was found that the external electric energy was very small compared

with the actual burning thermal energy of ethanol in this study. This was also mentioned in the

reference [22]. So the external energy by the electric field was considered insignificant and ignored

in the model.

Species:

$$\rho u \frac{\partial Y_i}{\partial x} + \rho v \frac{\partial Y_i}{\partial r} = -\frac{\partial \boldsymbol{J}_i}{\partial x} - \frac{1}{r}\frac{\partial (r\boldsymbol{J}_i)}{\partial r} + R_i + S_i \tag{6}$$

where Y_i is the mass fraction of species i, R_i is the net reaction rate, S_i is the additional

generation rate caused by source terms.

In order to simplify the calculation, a one-step chemical reaction model was used.

$$C_2H_5OH + 3O_2 = 2CO_2 + 3H_2O \tag{7}$$

The governing equations were solved using an implicit solver which is pressure based. The system

was closed with appropriate boundary conditions on each side of the computational domain. For the

small diffusion flame, the boundary conditions are consistent with the experimental condition, as

shown in Table 1. Identical boundary conditions were employed for the condition with electric field

and without electric field except for the electrode conditions. It was assumed that the purity of liquid

ethanol was 99.7%, the temperature of the liquid fuel applied was 300 K and the ethanol was

completely burnt. The model considered that the liquid ethanol had evaporated into gas near the

nozzle outlet. This is consistent with the actual experimental observation.

Table 1 Boundary conditions

Liquid ethanol inlet boundary condition	VEOCITY_INLET
Outlet boundary condition	PRESSURE_OUTLET
The wall of tube inside and outside	WALL
The electrodes condition	WALL

3.2 Numerical simulation and validation

The computational domain took the differences of the solid and the fluid zones into consideration,

which was divided into the ceramic tube solid zone, the fluid and combustion zone. A systematic grid independence test was carried out. The final mesh chosen had a total number of elements of 159980. Numerical simulations were performed for a reacting flow system with ethanol and air used as the fuel and oxidant respectively. In the simulation study, the oxygen mass fraction was taken as 23% (in ambient air). The ethanol was ignited above the burner nozzle outlet by assuming a temperature of 1000 K.

The accuracy of the present numerical model has been evaluated by comparing the measured and predicted flame shape and temperature. The small flame image captured by camera in the experiment and the flame temperature distribution of numerical calculation are shown in Fig. 4, respectively. Generally, in the high temperature region, the brightness of the flame will be high. So the flame image captured by camera and the calculated temperature field could indirectly reflect the flame shape. It was found that the flame shapes obtained from the two approaches were similar, which were both approximately spherical. Through the comparison of the flame temperature measured and calculated data, the difference between them was about 9%, and it is shown in Table 2. This was considered as acceptable. In addition, when the operating condition changed, the flame and temperature obtained by the measured results and calculated results both have the same trend of variation. It also implied the accuracy of the present numerical simulation.
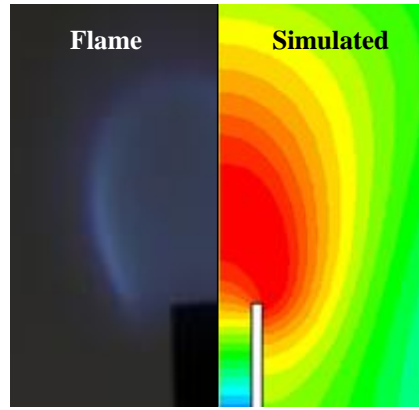
Fig. 4 Measured flame image and simulated temperature field without electric field (q_v=1.2 ml/h)

Table 2 Flame temperature and errors with flow rate of 1.2 ml/h

Temperature/K	no electric field	electric field
Experimental data	1326	1388
Numerical data	1446	1472
Discrepancies	9.0%	6.1%

4. Results and discussion

4.1 Velocity field

The flame of liquid ethanol in our small-scale combustor can only maintain stability within a certain range of fuel flow rates. When the fuel flow rate is too low or too high, the small flame cannot be ignited or will become oscillatory. In this study, the flame in a steady state was examined. The fuel flow rate of 1.2 ml/h where the flame could maintain stability was selected to perform the studies. Results about flow field of the flame were obtained. Fig. 5 shows the flow velocity vector diagrams near the flame without electric field and under positive electric field. Fig. 6 shows the comparison of flow field variations without and with the applied electric field. It was found that the velocity magnitude increased and the velocity changed more intensely when the electric field was applied.

This is mainly due to the influence of ionic wind [23]. There is a large number of positively and

14

negatively charged particles being produced by chemi-ionization in the hydrocarbon flame reaction

zone [30]. The positive electrode is below the flame and the negative electrode is above. These

charged particles would affect the combustion progress when the DC electric field was applied.

When the electric field was applied, the positively and negatively charged particles would move

toward the opposite polarity electrode by the force of electric field. Charged ions accelerated in the

electric field and transferred their momentum to the neutral molecules by colliding with them. With

the relatively small mean free path, the ions were accelerated by the electric field after each collision

[31], which produced a large number of neutral molecules moving toward the electrodes. The net

effect of this process is a significant body force produced by the electric field or the so-called "ionic

wind". In the same region, the flow velocity near the flame changed more intensely under the electric

field compared with the case without the electric field. It suggested that the velocity gradient is larger,

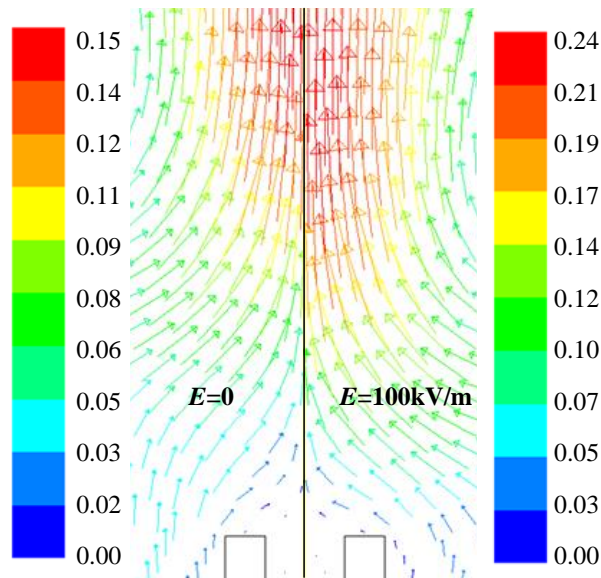which also indicated the existence of the electric field force as a source for the momentum [21].

Fig. 5 Calculated velocity field for the diffusion flame. Left: no electric field, right: $E= 100\,\text{kV/m}$
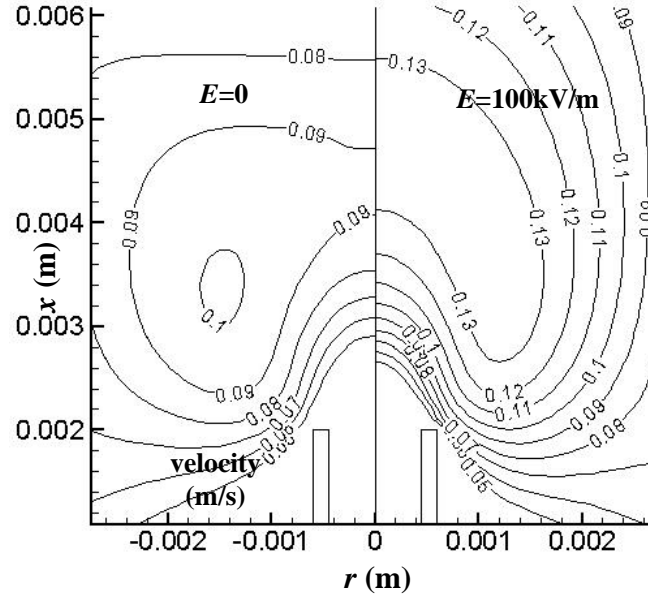
(q_v=1.2 ml/h)

Fig. 6 Calculated velocity contour. Left: no electric field, right: $E= 100$ kV/m (q_v=1.2 ml/h)

4.2 Mass fraction distribution

Obtained by numerical simulations, Fig. 7 and Fig. 8 show the ethanol and CO_2 mass fraction distributions, respectively. The effects of applied electric field on the species distribution can be observed. As seen from the figures, when the DC electric field was applied, the concentration of each species has a tendency of inward contraction. The increasing flow velocity near the flame due to the addition of electric field enhances the mixing of species. The applied electric field could increase the flame propagation velocity [18] and flame temperature by increasing the ion number density and redistributing the ion concentration, which enhances the combustion. The fuel rapidly spread to the air and met the oxidant and then the reaction took place. The fuel and oxidant burnt faster and were quickly consumed. The intensity of combustion process increased, and species distribution had an inward contraction.

A similar phenomenon can be seen from the calculated mass fraction profiles of O_2 and CO_2 on the axis as shown in Fig. 9. The maximum value of the mass fraction of CO_2 under positive electric field

was a little higher than that without the electric field and the point of maximum value moved

upstream. The mass fraction of O_2 also moved upstream and became more sharply decreasing close

to the flame. This observation agreed with the experimental results, which showed the reduction of

flame height with the increasing electric field strength. These results showed that the flame had a

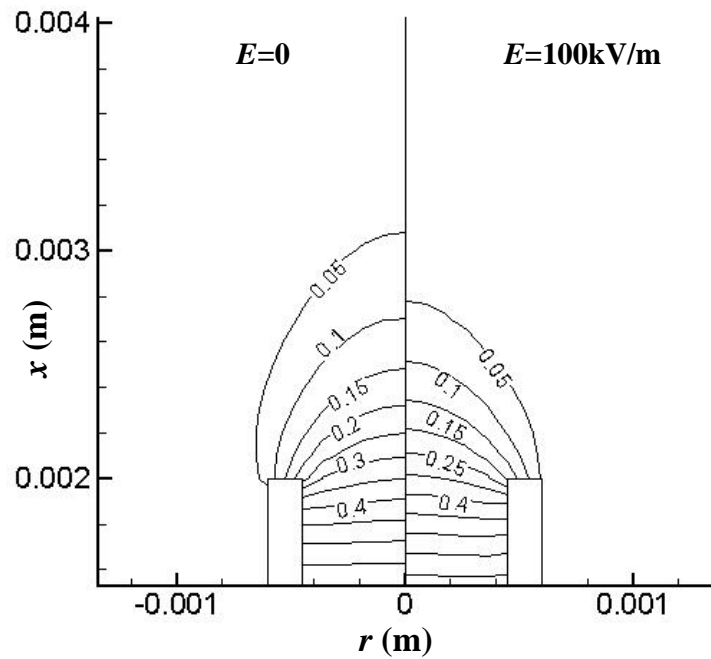tendency of contraction, which also implied the intensification of the reaction.

Fig. 7 Calculated ethanol mass fraction. Left: no electric field, right: $E= 100$ kV/m (q_v=1.2 ml/h)

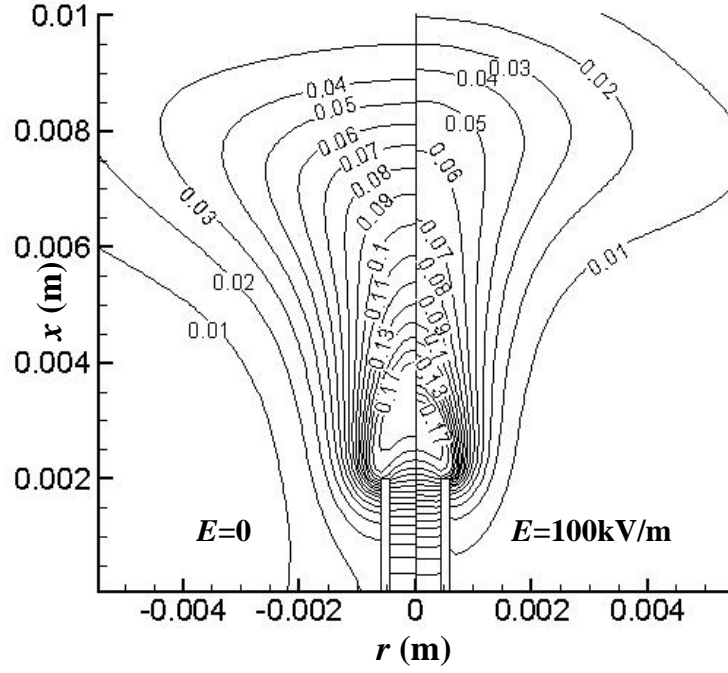Fig. 8 Calculated CO_2 mass fraction. Left: no electric field, right: $E=$ 100 kV/m (q_v=1.2 ml/h)
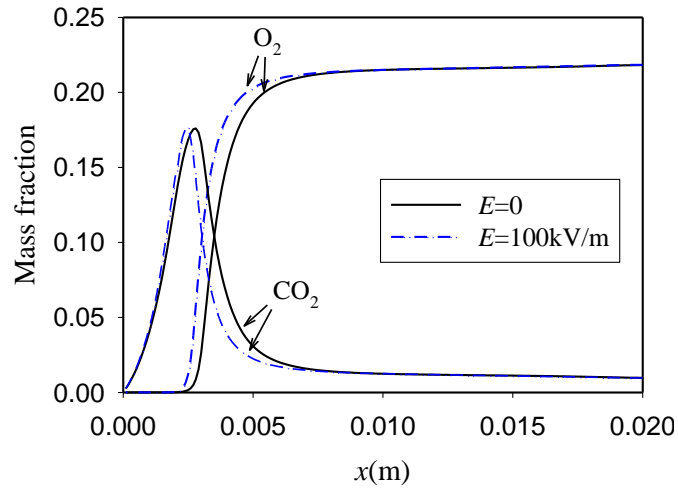

Fig. 9 Calculated mass fraction profiles of O_2 and CO_2 on the axis (q_v=1.2 ml/h)

4.3 Chemical reaction rate

From the numerical results, some changes in chemical reaction were observed when the electric

field was applied. Fig. 10 shows the chemical reaction rate in the flame. It can be found that when

the electric field was applied, the reaction rate in the flame increased and the scope of the reaction

expanded slightly. While the surface of chemical reactions has a tendency of contraction, which is

18

consistent with the mass fraction discussed before. It also suggests that the flame size decreases. It is known from the above that velocity close to the increased, which enhanced the fuel/oxygen mixing. The charged particles received an acceleration by electric field, which made charged particles mix quickly with oxygen in the flame front [10] and the reaction took place in a wider space. Thus, the reaction rate increased resulting in the fuel burning faster and the inward contraction of the flame front to the fuel side. It means that the DC electric field can enhance the combustion process and in turn lead to a higher flame temperature.
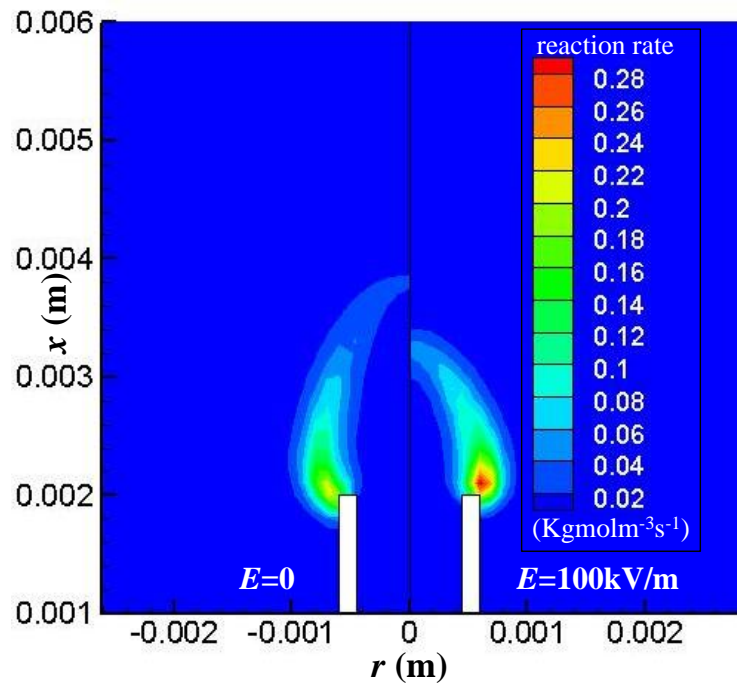

Fig. 10 Chemical reaction rate. Left: no electric field, right: $E= 100$ kV/m (q_v=1.2 ml/h)

4.4 Flame deformation in electric field

One important characteristic of laminar diffusion flame is the flame shape or structure. Fig. 11 shows the calculated temperature distribution of flame without electric field condition (left) and that under positive electric field (right) which also reflects the flame shape. Fuel flow rate was 1.2 ml/h, and the applied voltage was 4.0 kV (E=100 kV/m). It shows that the flame became shorter and

smaller after the electric field was applied. The flame height decreased by 50% with an applied
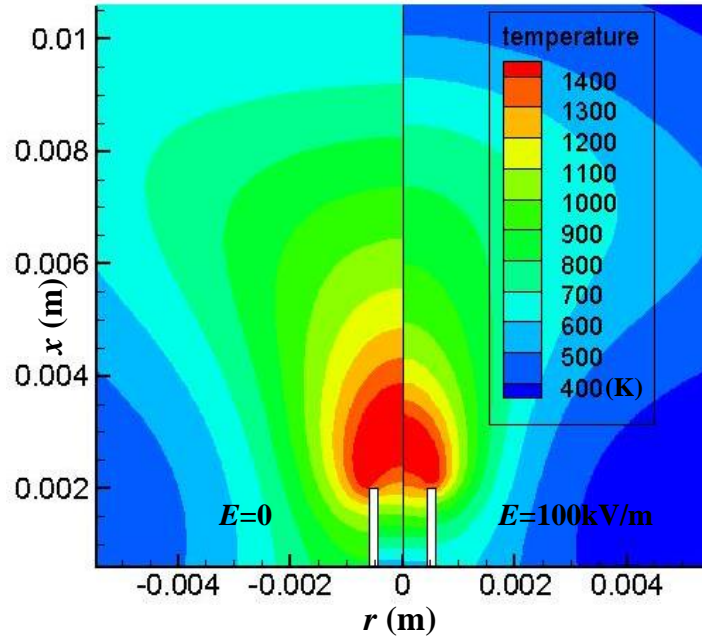
electric field.

Fig. 11 Calculated temperature fields. Left: no electric field, right: $E= 100$ kV/m (q_v=1.2 ml/h)

The maximum temperature with electric field appeared to be 1472 K which was slightly above (by

4.7%) the temperature with no electric field (1446 K). Owing to these aerodynamic effects associated

with the electrical field, the entire flow field is affected, and in particular the flame shape, which is

well known to be very sensitive to the surrounding flow field [32], is influenced accordingly. Thus,

the flame scale became smaller.

The aspect ratio was defined as the ratio of the flame height (H) to width (W)

$$\alpha = H/W \tag{8}$$

Fig. 12 shows the changes of flame deformation rate with the applied DC electric field strength

obtained from the experimental results. The results show a satisfactory correlation with the best fit of

the following equation with correlation coefficient R=0.9408.

$$\alpha = \frac{0.8983 - 0.0047E}{1 - 0.002E} \tag{9}$$

It could be found that the flame deformation rate became smaller with the increasing electric field strength. When the electric field strength was stronger, the electric field force was greater and the flame became flatter.

The flame shape is affected by the surrounding flow field, reaction rate and diffusion. The height of the laminar diffusion flame is proportional to the fuel flow rate, and is inversely proportional to the diffusion coefficient D. As known from the Fick's Diffusion Law, D is nearly proportional to $T^{3/2}$. According to the results of flame temperatures and discussions above, the flame temperature with applied electric field is higher than that without electric field. So the diffusivity increased and the flame became shorter under the effect of DC electric field. The electric field increased the flow velocity by the electric force and promoted the reaction rate and the diffusion of the species which also made the flame length shorter.
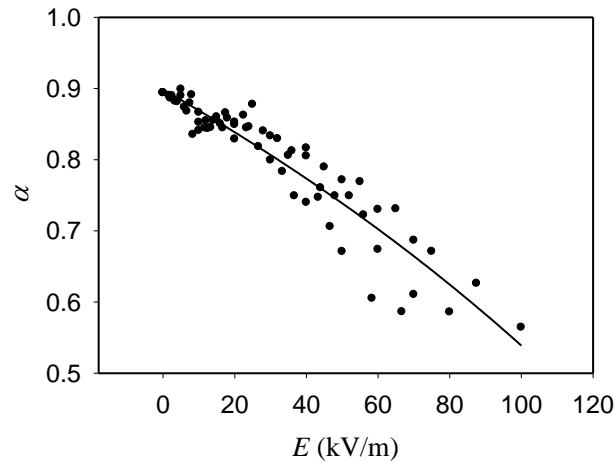

Fig. 12 The flame deformation rate with electric field strength collecting by experimental results

(q_v=1.2 ml/h)

5. Conclusions

The effects of DC electric field on the small ethanol diffusion flame were investigated. The flow velocity, chemical reaction rate, mass fraction distribution, flame temperature and deformation in the applied DC electric field were considered. The results show that the applied electric field changes the flame characteristics mainly due to the body forces acting on charged particles. The applied electric field accelerates the charged particles and they collide with the neutral particles and transfer the momentum, thus increasing the flow velocity. The effects on the species distribution and the flow field near the flame by the applied electric field promote the mixing of fuel and oxidant, which enhances the combustion process and leads to higher flame temperature. Flame becomes shorter with applied electric field and its deformation is related to the electric field strength.

References

[1] Ju Y, Maruta K. Microscale combustion: Technology development and fundamental research. Prog Energy Combust Sci 2011; 37(6): 669-715.

[2] Jun L, Yuantao W, Junrui S, Xueling L. Dynamic behaviors of premixed hydrogen-air flames in a planar micro-combustor filled with porous medium. Fuel 2015; 145: 70-78.

[3] Li J, Chou SK, Li ZW, Yang WM. Experimental investigation of porous media combustion in a planar micro-combustor. Fuel 2010; 89(3): 708-715.

[4] Gan YH, Luo ZB, Cheng YP, Xu JL. The electro-spraying characteristics of ethanol for application in a small-scale combustor under combined electric field. Appl Therm Eng 2015; 87: 595-604.

[5] Bagheri G, Hosseini SE, Wahid MA. Effects of bluff body shape on the flame stability in premixed micro-combustion of hydrogen–air mixture. Appl Therm Eng 2014; 67(1-2): 266-272.

[6] Tomcik P, Klaus P, Kulhanek J, Trojan R. Influence of electric field on stabilization of flame from poor methane-oxygen mixture. IEEE T Plasma Sci 2013; 41(8): 2230-2236.

[7] Maricq MM. The dynamics of electrically charged soot particles in a premixed ethylene flame. Combust Flame 2005; 141(4): 406-416.

[8] Maricq MM. Size and charge of soot particles in rich premixed ethylene flames. Combust Flame 2004; 137(3): 340-350.

[9] Xu KG. Plasma sheath behavior and ionic wind effect in electric field modified flames. Combust Flame 2014; 161(6): 1678-1686.

[10] Borgatelli F, Dunn-Rankin D. Behavior of a small diffusion flame as an electrically active component in a high-voltage circuit. Combust Flame 2012; 159(1): 210-220.

[11] Dae Geun P, Byung Chul C, Min Suk C, Suk Ho C. Soot reduction under DC electric fields in counterflow non-premixed laminar ethylene flames. Combust Sci Technol 2014; 186(4-5): 644-656.

[12] Wisman DL, Marcum SD, Ganguly BN. Electrical control of the thermodiffusive instability in premixed propane-air flames. Combust Flame 2007; 151(4): 639-648.

[13] Sakhrieh A, Lins G, Dinkelacker F, Hammer T, Leipertz A, Branston DW. The influence of pressure on the control of premixed turbulent flames using an electric field. Combust Flame 2005; 143(3): 313-322.

[14] Marcum SD, Ganguly BN. Electric-field-induced flame speed modification. Combust Flame 2005; 143(1-2): 27-36.

[15] Ata A, Cowart JS, Vranos A, Cetegen BM. Effects of direct current electric field on the blowoff characteristics of bluff-body stabilized conical premixed flames. Combust Sci Technol 2005; 177(7): 1291-1304.

[16] Giorgi MGD, Sciolti A, Campilongo S, Pescini E, Ficarella A, Martini LM, Tosi P, Dilecce G. Plasma assisted flame stabilizationin a non-premixed lean burner. Energy Procedia 2015; 82: 410-416.

[17] Zhang Y, Wu YX, Yang HR, Zhang H, Zhu M. Effect of high-frequency alternating electric fields on the behavior and nitric oxide emission of laminar non-premixed flames. Fuel 2013; 109: 350-355.

[18] Meng XW, Wu XM, Kang C, Tang AD, Gao ZQ. Effects of Direct-Current (DC) electric fields on flame propagation and combustion characteristics of premixed $CH_4/O_2/N_2$ flames. Energy Fuels 2012; 26(11): 6612-6620.

[19] Imamura O, Chen B, Nishida S, Yamashita K, Tsue M, Kono M. Combustion of ethanol fuel droplet in vertical direct current electric field. Proc Combust Inst 2011; 33(2): 2005-2011.

[20] Imamura O, Yamashita K, Nishida S, Ianus G, Tsue M, Kono M. Two-droplet combustion of n-octane in a direct current electric field under microgravity. Combust Sci Technol 2011; 183(8): 755-763.

[21] Kim MK, Ryu SK, Won SH, Chung SH. Electric fields effect on liftoff and blowoff of nonpremixed laminar jet flames in a coflow. Combust Flame 2010; 157(1): 17-24.

[22] van den Boom JDBJ, Konnov AA, Verhasselt AMHH, Kornilov VN, de Goey LPH, Nijmeijer H.

The effect of a DC electric field on the laminar burning velocity of premixed methane/air flames. Proc Combust Inst 2009; 32(1): 1237-1244.

[23] Belhi M, Domingo P, Vervisch P. Modelling of the effect of DC and AC electric fields on the stability of a lifted diffusion methane/air flame. Combust Theor Model 2013; 17(4): 749-787.

[24] Won SH, Cha MS, Park CS, Chung SH. Effect of electric fields on reattachment and propagation speed of tribrachial flames in laminar coflow jets. Proc Combust Inst 2007; 31: 963-970.

[25] Karnani S, Dunn-Rankin D. Detailed characterization of DC electric field effects on small non-premixed flames. Combust Flame 2015; 162(7): 2865-2872.

[26] Vega EV, Shin SS, Lee KY. NO emission of oxygen-enriched $CH_4/O_2/N_2$ premixed flames under electric field. Fuel 2007; 86(4): 512-519.

[27] Gan YH, Xu JL, Yan YY, Wang M, Luo YL, Yang ZL. A comparative study on free jet and confined jet diffusion flames of liquid ethanol from small nozzles. Combust Sci Technol 2014; 186(2): 120-138.

[28] Gan YH, Wang M, Luo YL, Chen XW, Xu JL. Effects of direct-current electric fields on flame shape and combustion characteristics of ethanol in small scale. Adv Mech Eng 2016; 8(1): 1-14.

[29] Gan YH, Luo YL, Wang M, Shi YL, Yan YY. Effect of alternating electric fields on the behaviour of small-scale laminar diffusion flames. Appl Therm Eng 2015; 89: 306-315.

[30] Weinberg FJ, Dunn-Rankin D, Carleton FB, Karnani S, Markides C, Zhai M. Electrical aspects of flame quenching. Proc Combust Inst 2013; 34: 3295-3301.

[31] Lawton J, Weinberg FJ, electrical aspects of combustion, Clarendon Press, Oxford, 1969.

[32] Hu J, Rivin B, Sher E. The effect of an electric field on the shape of co-flowing and candle-type methane-air flames. Exp Therm Fluid Sci 2000; 21(1-3): 124-133.

1 **List of figure captions**

2 Fig. 1 Experimental system

3 Fig. 2 Flame temperature measuring point

4 Fig. 3 The configuration studied

5 Fig. 4 Measured flame image and simulated temperature field without electric field (q_v=1.2 ml/h)

6 Fig. 5 Calculated velocity field for the diffusion flame. Left: no electric field, right: E= 100 kV/m

7 (q_v=1.2 ml/h)

8 Fig. 6 Calculated velocity contour. Left: no electric field, right: E= 100 kV/m (q_v=1.2 ml/h)

9 Fig. 7 Calculated ethanol mass fraction. Left: no electric field, right: E= 100 kV/m (q_v=1.2 ml/h)

10 Fig. 8 Calculated CO_2 mass fraction. Left: no electric field, right: E= 100 kV/m (q_v=1.2 ml/h)

11 Fig. 9 Calculated mass fraction profiles of O_2 and CO_2 on the axis (q_v=1.2 ml/h)

12 Fig. 10 Chemical reaction rate. Left: no electric field, right: E= 100 kV/m (q_v=1.2 ml/h)

13 Fig. 11 Calculated temperature fields. Left: no electric field, right: E= 100 kV/m (q_v=1.2 ml/h)

14 Fig. 12 The flame deformation rate with electric field strength collecting by experimental results

15 (q_v=1.2 ml/h)